2021 IEEE Conference on Control Technology and Applications (CCTA).
August 8-11, 2021. San Diego, California

2021 IEEE Conference on Control Technology and Applications (CCTA).
August 8-11, 2021. San

Cluster Formation in Multiagent Consensus via Dynamic Resilient Graph Games

Yurid Nugraha, Ahmet Cetinkaya, Tomohisa Hayakawa, Hideaki Ishii, and Quanyan Zhu

2021 IEEE Conference on Control Technology and Applications (CCTA) | 978-1-6654-3643-4/21/$31.00 ©2021 IEEE | DOI: 10.1109/CCTA48906.2021.9659182

Abstract— **In this paper we formulate a two-player game-theoretic problem on resilient graphs representing communication channels that are vulnerable to attacks in multiagent consensus setting. An attacker is capable to disconnect part of the edges of the graph by emitting jamming signals while, in response, the defender recovers some of them by increasing the transmission power for the communication signals over the corresponding edges. It is also possible for the attacker to emit stronger jamming signals that cannot be overcome by the defender. We consider repeated games where the utilities of players in each game depend on attack/recovery performance measured over multiple intervals. The utilities of both players are mainly related to agents' states and the cluster formation, i.e., how the agents are divided. The players' actions are constrained by their energy for transmissions, with a less strict constraint for the attacker compared to the defender. Numerical examples of dynamic games played over time are provided to demonstrate the cluster formation.**

I. Introduction

Applications of large-scale networked systems have rapidly grown in various areas of critical infrastructures including power grid and transportation systems. Such systems can be considered as multiagent systems where a number of agents capable of making local decisions interact over a network and exchange information [1]. While wireless communication plays an important role to the functionality of the network, it is also prone to cyber attacks initiated by adversaries on the networked systems [2]. For instance, wireless communication among agents can be easily interrupted by means of jamming attacks that do not require prior knowledge of the network.

Noncooperative game theory is widely used for addressing security problems [3], [4] while jamming attacks on consensus problems of multiagent systems have also been studied. For example, the work [5] incorporates the jamming attack models with energy constraints studied in [6]–[8] for networked control problems. However, optimal strategies for such attacks and defenses in consensus problems have not been well addressed.

In this paper, we model the interaction between an attacker and a defender in a two-player game setting played repeatedly over time in the context of multiagent consensus. The attacker is motivated to disrupt the communication among agents by attacking individual links while the defender attempts to recover some or all of them whenever possible. Their utilities are determined by how agents are connected to others during the attacks and recoveries, as well as how these actions affect the states of agents. Both players are constrained in terms of their available energy for the actions of attacks/recoveries.

We formulate the problem based on our recent work [9], which uses graph connectivity to characterize the game and players' strategies (see also [10]). Specifically, we address how clusters among agents may form in this security game setting. Cluster formation in multiagent systems has been studied in, e.g., [11], [12], where the weights in the agents' state updates may take negative values, representing the possibly hostile relations among certain agents. In this paper, we approach clustering from a different viewpoint based on a game-theoretic formulation. Moreover, different from [9], [10], (i) we introduce more options for the attacker's attack strengths and (ii) the game consists of multiple parts, resulting in more complicated attack/defense strategies.

More specifically, with different attack strengths, it is now possible for the attacker to attack the links with stronger attack signals so that the defender is unable to recover those links. In practice, this is possible when the attacker emits stronger jamming signals to particular communication links that results in much lower signal-to-interference-plus-noise ratio (SINR) so that it is not possible for the defender to recover the communication on those links with its limited resources. Such models are employed in [13], [14].

On the other hand, we consider games consisting of multiple parts, where the players need to consider their future conditions when deciding their strategies at any point in time. This has an impact on how the players use their limited energy; it may be possible that the players reduce their intensity of attack/recovery actions at some time to conserve their energy and use it more efficiently later.

The paper is organized as follows. In Section II, we introduce the framework for the resilient graph game. In Section III, we discuss the effect of some of the parameters on the equilibria and cluster formation. We provide a case study to analyze the better strategies for players in one game in Section IV. We then present simulations on the dynamic graph games and the resulting cluster formation in Section V. Finally, we conclude the paper in Section VI.

Yurid Nugraha and Tomohisa Hayakawa are with the Department of Systems and Control Engineering, Tokyo Institute of Technology, Tokyo 152-8552, Japan. yurid@dsl.sc.e.titech.ac.jp, hayakawa@sc.e.titech.ac.jp

Ahmet Cetinkaya is with the Information Systems Architecture Science Research Division, National Institute of Informatics, Tokyo 101-8430, Japan. cetinkaya@nii.ac.jp

Hideaki Ishii is with the Department of Computer Science, Tokyo Insitute of Technology, Yokohama 226-8502, Japan. ishii@c.titech.ac.jp

Quanyan Zhu is with the Department of Electrical and Computer Engineering, New York University, Brooklyn NY, 11201, USA. quanyan.zhu@nyu.edu

This work was supported in part by the JST CREST Grant No. JPMJCR15K3, by JST ERATO HASUO Metamathematics for Systems Design Project (No. JPMJER1603), by JSPS KAKENHI Grant Numbers 20K14771 and 18H01460, and by National Science Foundation (NSF) under Grants CNS-1544782 and ECCS-1847056.

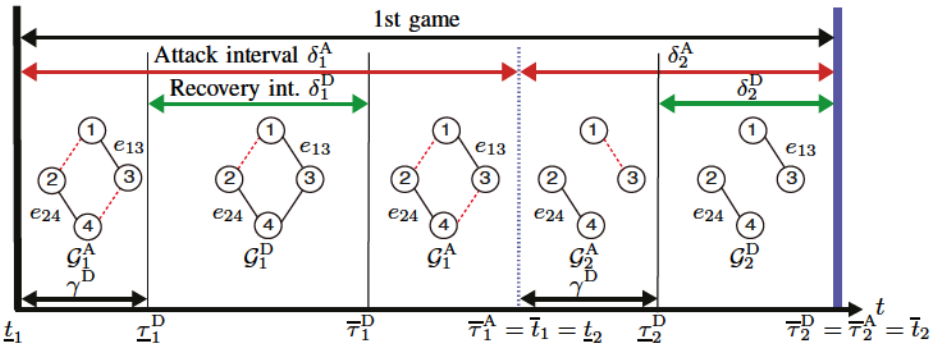

Fig. 1. Illustration of graph transitions, with $\mathcal{G}$ containing four edges $e_{12}, e_{13}, e_{24}, e_{34}$. A game consists of two attack parts. The blue dashed line indicates the end of the first part, while the blue solid line the end of the second part (and hence the game). In the graphs, the solid and dashed lines indicate edges connected and disconnected, respectively; no lines in e_{12} and e_{24} in the second part indicate that those edges are attacked strongly.

All the proofs are omitted due to space limitations.

II. Problem Formulation

In this section, we explain the two-player game formulation between an attacker and a defender in the context of network security. We also explain the characteristics of the players, such as their energy constraints and how they measure the cluster formation of the agents.

We consider a multiagent system consisting of n agents with the communication topology described by the graph $\mathcal{G} = (\mathcal{V}, \mathcal{E})$, where the set $\mathcal{V}$ of vertices representing the agents and the set $\mathcal{E} \subseteq \mathcal{V} \times \mathcal{V}$ of edges representing the communication links between the agents. Every agent i is able to communicate with its neighbors $\mathcal{N}_i(t) \subseteq \mathcal{V}$ via the communication links. The underlying graph $\mathcal{G}$, which is undirected and connected, represents the communication topology when there are no attacks.

Each agent has the scalar state x_i whose dynamics are given by

$$\dot{x}_i(t) = \sum_{j \in \mathcal{N}_i(t)} (x_j(t) - x_i(t)), \quad x(0) = x_0, \quad t \geq 0. \tag{1}$$

Under the dynamics (1), all agents are expected to converge towards the same state as time progresses as long as the communication topology is connected.

In this paper, we consider the two-player game between the attacker and the defender on how the agents communicate with each other in a networked system vulnerable to jamming attacks. The attacker blocks the communication by sending jamming signals, whereas the defender recovers some of the attacked links by asking agents to send stronger communication signals on those links. In particular, the attacker has two types of jamming signals in terms of their strength, *strong* and *normal*. We define the attack action by the attacker (both with strong and normal signals) as the removal of edges in graph $\mathcal{G}$. In response to the attacks, the recovery action by the defender is represented by restoring some of the removed edges. The difference between the two jamming signal types is that the edges attacked with strong jamming signals cannot be recovered. The two types of attacks can be made simultaneously on different edges.

A. Attack-Recovery Sequence

The players decide whether to attack/recover in the time interval $[\underline{t}_k, \overline{t}_k]$, with $k \in \mathbb{N}$ and $\overline{t}_k > \underline{t}_k = \overline{t}_{k-1}$. At $\underline{t}_k$, the system is represented by the original graph $\mathcal{G}$. Then, the players may start attacking and recovering certain links sequentially, with the attacker acting before the defender. The attack/recovery durations and the links for the attack/recovery are the action variables to be decided by the players. In this game, the players can make their actions at most once in $[\underline{t}_k, \overline{t}_k]$. Once the attacker stops the attacks (and therefore also ending all recovery attempts), the kth interval ends at $\overline{t}_k$. The next interval then immediately begins, that is, $\underline{t}_{k+1} = \overline{t}_k$.

More specifically, the attacker attacks $\mathcal{G}$ by deleting $\mathcal{E}_k^{\mathrm{A}} \subseteq \mathcal{E}$ (normal jamming signals) and $\bar{\mathcal{E}}_k^{\mathrm{A}} \subseteq \mathcal{E}$ (strong jamming signals) with $\mathcal{E}_k^{\mathrm{A}} \cap \bar{\mathcal{E}}_k^{\mathrm{A}} = \emptyset$ from time $\underline{t}_k$ until $\overline{\tau}_k^{\mathrm{A}}$, whereas the defender recovers $\mathcal{E}_k^{\mathrm{D}} \subseteq \mathcal{E}_k^{\mathrm{A}}$ from $\underline{\tau}_k^{\mathrm{D}}$ until $\overline{\tau}_k^{\mathrm{D}}$, with $\underline{t}_k < \underline{\tau}_k^{\mathrm{D}} \leq \overline{\tau}_k^{\mathrm{D}} \leq \overline{t}_k$. Because of the presence of the attacks, $\mathcal{G}$ is changed to $\mathcal{G}_k^{\mathrm{A}} := (\mathcal{V}, \mathcal{E} \setminus (\bar{\mathcal{E}}_k^{\mathrm{A}} \cup \mathcal{E}_k^{\mathrm{A}}))$ beginning from $\underline{t}_k$. Similarly, because of the recovery action by the defender, $\mathcal{G}_k^{\mathrm{A}}$ is changed to $\mathcal{G}_k^{\mathrm{D}} := (\mathcal{V}, (\mathcal{E} \setminus (\bar{\mathcal{E}}_k^{\mathrm{A}} \cup \mathcal{E}_k^{\mathrm{A}}) \cup \mathcal{E}_k^{\mathrm{D}})$ from $\underline{\tau}_k^{\mathrm{D}}$ until $\overline{\tau}_k^{\mathrm{D}}$. The graph $\mathcal{G}_k^{\mathrm{D}}$ changes back to $\mathcal{G}_k^{\mathrm{A}}$ from $\overline{\tau}_k^{\mathrm{D}}$ to $\overline{\tau}_k^{\mathrm{A}}$, if the defender ends its recovery before the attacker ends its attack. Otherwise, the defender can only recover until $\overline{\tau}_k^{\mathrm{A}}$, i.e., $\overline{\tau}_k^{\mathrm{A}} = \overline{\tau}_k^{\mathrm{D}}$. The graph becomes $\mathcal{G}$ again when the attacker stops jamming, as the new $(k+1)$th interval begins. For attacking/recovering links, both players spend energy in proportion to the attack/recovery duration. In this formulation, we consider a constant waiting time (representing the time needed for the defender to recognize the attack) $\gamma^{\mathrm{D}} \geq 0$ between $\underline{t}_k$ and $\underline{\tau}_k^{\mathrm{D}}$, unless the attacker ends attacking earlier, which is specified by $\underline{\tau}_k^{\mathrm{D}} = \min(\overline{\tau}_k^{\mathrm{A}}, \underline{t}_k + \gamma^{\mathrm{D}})$. The attack and recovery durations denoted respectively by δ_k^{A} and δ_k^{D}, are given as

$$\delta_k^{\mathrm{A}} := \overline{\tau}_k^{\mathrm{A}} - \underline{t}_k, \quad \delta_k^{\mathrm{D}} := \overline{\tau}_k^{\mathrm{D}} - \underline{\tau}_k^{\mathrm{D}}. \tag{2}$$

The end time $\overline{t}_k$ of the kth interval is specified by

$$\overline{t}_k := \begin{cases} \overline{\tau}_k^{\mathrm{A}}, & \text{if } (\bar{\mathcal{E}}_k^{\mathrm{A}} \cup \mathcal{E}_k^{\mathrm{A}}) \neq \emptyset, \\ \underline{t}_k + \gamma^{\mathrm{D}}, & \text{otherwise.} \end{cases} \tag{3}$$

This indicates that the attacker ends the game at the end of a nonzero attack interval. Otherwise, the attacker does not attack, in which case the game ends at $\underline{t}_k + \gamma^{\mathrm{D}}$.

In this game, players attempt to choose the best strategies in terms of edges attacked/recovered and attack/recovery durations $((\bar{\mathcal{E}}_k^{\mathrm{A}}, \mathcal{E}_k^{\mathrm{A}}, \delta_k^{\mathrm{A}})$ and $(\mathcal{E}_k^{\mathrm{D}}, \delta_k^{\mathrm{D}}))$ to maximize their own utility functions of the game defined over multiple intervals. Specifically, in this paper we consider the simplest case, which is the game defined over two intervals $[\underline{t}_k, \overline{t}_k]$ and $[\underline{t}_{k+1}, \overline{t}_{k+1}]$ as explained in Section II-D below.

Fig. 1 illustrates the sequences of the attack and recovery actions described so far. In this figure, the attacker attacks e_{12} and e_{34} in $[\underline{t}_1, \overline{t}_1]$, but the defender recovers one of them. The attacker attacks different edges with different attack strength in $[\underline{t}_2, \overline{t}_2]$, and the defender can only recover

e_{13}, which is attacked normally. The attacker ends attacking before the defender ends recovering in the second interval in this example, and therefore the interval ends at $\overline{\tau}_2^{\mathrm{D}} = \overline{\tau}_2^{\mathrm{A}}$.

B. Energy Constraints

In this formulation, the players cannot keep sending signals to all edges for infinite duration due to the energy constraints [6], [9], where players have some initial energy and are able to recharge their energy over time. Here, the attacker has two types of jamming signals. The strong attacks on $\bar{\mathcal{E}}_k^{\mathrm{A}}$ take $s > 1$, $s \in \mathbb{R}$, times more energy per edge per unit time compared to the normal attacks on $\mathcal{E}_k^{\mathrm{A}}$. In our numerical examples and analysis, we consider the case where $s = 2$, i.e., attacking an edge strongly takes twice the energy. The attacker's energy usage is constrained as

$$\sum_{m=1}^{k-1} \beta^{\mathrm{A}}(s|\bar{\mathcal{E}}_m^{\mathrm{A}}|+|\mathcal{E}_m^{\mathrm{A}}|)\delta_m^{\mathrm{A}} + \beta^{\mathrm{A}}(s|\bar{\mathcal{E}}_k^{\mathrm{A}}|+|\mathcal{E}_k^{\mathrm{A}}|)(t-\underline{t}_k) \leq \kappa^{\mathrm{A}} + \rho^{\mathrm{A}} t, \tag{4}$$

for any $t \in [\underline{t}_k, \underline{t}_{k+1}]$, with $\kappa^{\mathrm{A}} \geq 0$, $\beta^{\mathrm{A}} > 0$, and $\beta^{\mathrm{A}}|\mathcal{E}| > \rho^{\mathrm{A}} > 0$. The parameters κ^{A}, ρ^{A}, and β^{A} denote the attacker's initial energy, its recharge rate, and its unit cost of attacking one edge per time, respectively.

Since from (4) it is possible that $\rho^{\mathrm{A}} > \beta^{\mathrm{A}}$, i.e., the attacker recharges its energy faster than it consumes, the attacker can attack up to a certain number of edges for infinite time. We denote that number of edges as $\bar{m}^{\mathrm{A}} := \lfloor \rho^{\mathrm{A}}/\beta^{\mathrm{A}} \rfloor$, where the attacker can attack edges $\bar{\mathcal{E}}_k^{\mathrm{A}}$ and $\mathcal{E}_k^{\mathrm{A}}$ satisfying $s|\bar{\mathcal{E}}_k^{\mathrm{A}}|+|\mathcal{E}_k^{\mathrm{A}}| \leq \bar{m}^{\mathrm{A}}$ for infinite duration. Otherwise, we obtain the maximum attack duration Δ_k^{A} where the left-hand side of (4) is equal to the right-hand side as

$$\Delta_k^{\mathrm{A}} := \frac{\kappa^{\mathrm{A}} + \beta^{\mathrm{A}}(s|\bar{\mathcal{E}}_k^{\mathrm{A}}|+|\mathcal{E}_k^{\mathrm{A}}|)\underline{t}_k}{\beta^{\mathrm{A}}(s|\bar{\mathcal{E}}_k^{\mathrm{A}}|+|\mathcal{E}_k^{\mathrm{A}}|) - \rho^{\mathrm{A}}} - \frac{\sum_{m=1}^{k-1} \beta^{\mathrm{A}}(s|\bar{\mathcal{E}}_m^{\mathrm{A}}|+|\mathcal{E}_m^{\mathrm{A}}|)\delta_m^{\mathrm{A}}}{\beta^{\mathrm{A}}(s|\bar{\mathcal{E}}_k^{\mathrm{A}}|+|\mathcal{E}_k^{\mathrm{A}}|) - \rho^{\mathrm{A}}} - \underline{t}_k. \tag{5}$$

This energy consumption model for the attacker is illustrated in Fig. 2, where the black dashed line with slope ρ^{A} represents the right-hand side of (4) and the black solid line with slope $\beta^{\mathrm{A}}(s|\bar{\mathcal{E}}_k^{\mathrm{A}}|+|\bar{\mathcal{E}}_k^{\mathrm{A}}|)$ represents the actual energy consumed by the attacker, shown in the left-hand side in (4). The attacker runs out of energy when the solid line touches the dashed line. It is then possible for the attacker to never run out of energy if the dashed line is steeper than the solid line, i.e., the attacker attacks only a few edges so that $\beta^{\mathrm{A}}(s|\bar{\mathcal{E}}_k^{\mathrm{A}}|+|\mathcal{E}_k^{\mathrm{A}}|) \leq \rho^{\mathrm{A}}$. However, the attacker may want to maximize the damage on the system by attacking more/stronger edges in some attack intervals. In the game structure explained later, we consider the scenarios where the attacker always attacks more edges and hence runs out of energy every two attack intervals, as also illustrated in Fig. 2 where the energy consumed by the attacker reaches the limit at the end of every δ_k^{A} with even k.

Similar to (4), the defender's constraint is given by

$$\sum_{m=1}^{k-1} \beta^{\mathrm{D}}|\mathcal{E}_m^{\mathrm{D}}|\delta_m^{\mathrm{D}} + \beta^{\mathrm{D}}|\mathcal{E}_k^{\mathrm{D}}|(t-\underline{\tau}_k^{\mathrm{D}}) \leq \kappa^{\mathrm{D}} + \rho^{\mathrm{D}} t, \tag{6}$$

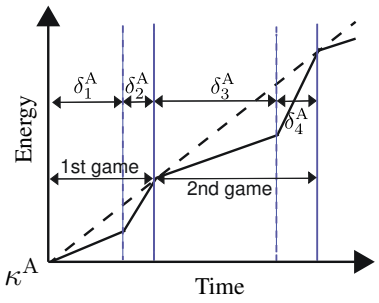

Fig. 2. The attacker's energy consumption model, with $\kappa^{\mathrm{A}} = 0$. The vertical blue lines indicate the end time of each attack interval: dashed lines for the end of the first parts and solid lines for the second parts.

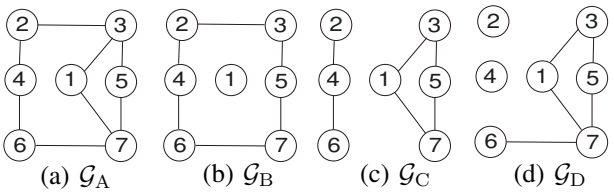

Fig. 3. Graphs and their cluster distributions: (a) $c(\mathcal{G}_{\mathrm{A}}) = 0$, (b) $c(\mathcal{G}_{\mathrm{B}}) = -12$, (c) $c(\mathcal{G}_{\mathrm{C}}) = -24$, and (d) $c(\mathcal{G}_{\mathrm{D}}) = -22$. Note that $c(\mathcal{G}_{\mathrm{D}})$ is larger than $c(\mathcal{G}_{\mathrm{C}})$, even with more clusters.

for any $t \in [\underline{\tau}_k^{\mathrm{D}}, \underline{\tau}_{k+1}^{\mathrm{D}}]$, with $\kappa^{\mathrm{D}} > 0$ and $\beta^{\mathrm{D}} > \rho^{\mathrm{D}} > 0$. We also obtain Δ_k^{D} similar to (5) above.

C. Agent Clustering and State Difference

By attacking, the attacker makes the graph disconnected and in turn separates the agents into clusters. Specifically, in a given graph $\mathcal{G}'$, the agents are grouped into $\tilde{c}(\mathcal{G}')$ clusters, with the clusters $\mathcal{V}_1^{\mathcal{G}'}, \mathcal{V}_2^{\mathcal{G}'}, \ldots, \mathcal{V}_{\tilde{c}(\mathcal{G}')}^{\mathcal{G}'}$ being a partition of $\mathcal{V}$ with $\cup_{l=1}^{\tilde{c}(\mathcal{G}')} \mathcal{V}_l^{\mathcal{G}'} = \mathcal{V}$ and $\mathcal{V}_l^{\mathcal{G}'} \cap \mathcal{V}_m^{\mathcal{G}'} = \emptyset,\ l \neq m$.

Here, we are interested in the case where the attacker is also concerned about the number of agents in each cluster, as an extension of [9]. Specifically, we follow the notion of *network effect/externality* [15], where the utility of an agent in a certain cluster depends on how many other agents belong to that particular cluster. In the context of this game, the attacker does not want too many agents to be together in the same cluster in order to minimize the spread of information. Hence, the distribution of agents among clusters becomes important. For example, if there are 12 agents, the attacker can choose to: 1) separate the agents into 3 clusters with ten agents in cluster 1 and one agent each in both clusters 2 and 3, or 2) separate into two clusters with both clusters 1 and 2 consisting of six agents each. The option 2) may be better than 1) for the attacker despite having fewer clusters, because the agents are distributed more evenly so that most of them are not grouped together in the same cluster.

Motivated by the example above, here we define the cluster distributions $c(\cdot)$ as

$$c(\mathcal{G}') := \sum_{l=1}^{\tilde{c}(\mathcal{G}')} |\mathcal{V}_l^{\mathcal{G}'}|^2 - n^2 (\leq 0). \tag{7}$$

The value of $c(\mathcal{G}')$ is 0 if $\mathcal{G}'$ is connected, since there is only one cluster. A larger value (closer to 0) of $c(\mathcal{G}')$ implies that there are fewer clusters in graph $\mathcal{G}'$, with each cluster having more agents. The cluster distributions of some graphs are shown in Fig. 3. Here, it is interesting that $c(\mathcal{G}_{\mathrm{C}})$ is smaller than $c(\mathcal{G}_{\mathrm{D}})$, even though $\mathcal{G}_{\mathrm{D}}$ has more clusters. Thus, for an

attacker who tries to reduce the number of agents grouped together in one cluster, $\mathcal{G}_{\mathrm{C}}$ is preferable to $\mathcal{G}_{\mathrm{D}}$.

In this setting the players also consider the effects of their actions on the agent states when attacking/recovering, similar to the formulation in [16]. For example, the attacker may want to separate agents having state values with more difference in different clusters. We specify the agents' state difference z_k of the kth interval as

$$z_k((\bar{\mathcal{E}}_k^{\mathrm{A}}, \mathcal{E}_k^{\mathrm{A}}, \delta_k^{\mathrm{A}}), (\mathcal{E}_k^{\mathrm{D}}, \delta_k^{\mathrm{D}})) := x^{\mathrm{T}}(\bar{t}_k) L_{\mathrm{c}} x(\bar{t}_k), \quad (8)$$

with L_{c} being the Laplacian matrix of the complete graph with n agents. Note that the value of z_k does not increase over time [1].

D. Two-interval Game Structure

The players' utility functions of the lth game over $[\underline{t}_{2l-1}, \bar{t}_{2l}]$ take account of the cluster distribution $c(\cdot)$ and the difference $z_k(\cdot,\cdot)$ of agents' states, and are defined by

$$U^{\mathrm{A}} := \sum_{k=2l-1}^{2l} a z_k \delta_k^{\mathrm{A}} - b(c(\mathcal{G}_k^{\mathrm{A}})(\delta_k^{\mathrm{A}} - \delta_k^{\mathrm{D}}) + c(\mathcal{G}_k^{\mathrm{D}})\delta_k^{\mathrm{D}}), \quad (9)$$

$$U^{\mathrm{D}} := -U^{\mathrm{A}}, \quad (10)$$

where $a, b > 0$. These utility functions represent the number of clusters over attack duration for two consecutive attack intervals, since the attacker's energy runs out after the two attack intervals as explained above. The players change their strategies once during the two intervals, i.e., once in a game. These strategies are determined at the beginning of each game, as explained later. From now on, we refer to these two attack intervals as two parts of the lth game.

From the discussion on the energy constraint in Section II-B, it is possible that the attacker never runs out of energy if the attacked edges $\bar{\mathcal{E}}_k^{\mathrm{A}}$ and $\mathcal{E}_k^{\mathrm{A}}$ satisfy $(s|\bar{\mathcal{E}}_k^{\mathrm{A}}|+|\mathcal{E}_k^{\mathrm{A}}|) \leq \bar{m}^{\mathrm{A}}$. Since there is no maximum attack duration Δ_k^{A}, in this case we suppose that the choices for attack duration are limited to $\delta_k^{\mathrm{A}} \in \{\delta/2, \delta\}$ for simplicity, with constant $\delta > 2\gamma^{\mathrm{D}} > 0$.

In this setting, we assume that in the $(2l-1)$th attack interval (the first part of the lth game) the attacker attacks edges $\bar{\mathcal{E}}_{2l-1}^{\mathrm{A}}$ and $\mathcal{E}_{2l-1}^{\mathrm{A}}$ satisfying $(s|\bar{\mathcal{E}}_{2l-1}^{\mathrm{A}}|+|\mathcal{E}_{2l-1}^{\mathrm{A}}|) \leq \bar{m}^{\mathrm{A}}$, with the choices of $\delta_{2l-1}^{\mathrm{A}} \in \{\delta/2, \delta\}$ specified above. In the next $(2l)$th interval (the second part of the game), we suppose that the attacker chooses to attack $\bar{\mathcal{E}}_{2l}^{\mathrm{A}}$ and $\mathcal{E}_{2l}^{\mathrm{A}}$ satisfying $(s|\bar{\mathcal{E}}_{2l}^{\mathrm{A}}|+|\mathcal{E}_{2l}^{\mathrm{A}}|) > \bar{m}^{\mathrm{A}}$, i.e., more/stronger edges than in the first part, for finite Δ_{2l}^{A} duration as in (5), i.e., $\delta_{2l}^{\mathrm{A}} = \Delta_{2l}^{\mathrm{A}}$. Therefore, we have two intervals with different characteristics in each lth game. For simplicity, in this game the defender is only able to recover until either it runs out of energy, or the recovery is interrupted by the stoppage of the attack, i.e., $\delta_k^{\mathrm{D}} \in \{0, \min\{\delta_k^{\mathrm{A}} - \gamma^{\mathrm{D}}, \Delta_k^{\mathrm{D}}\}\}, k \in \mathbb{N}$.

The players determine their actions based on the subgame perfect equilibrium concept, as in [9]. In order to find the equilibrium, the game is classified into some subgames/decision-making points. The subgame perfect equilibrium must be an equilibrium in every subgame. The optimal strategy of each player is obtained by using a backward induction approach, i.e., by finding the equilibrium from smallest subgames. The subgame perfect equilibrium solution concept is suitable for this problem setting, since players decide their strategies in a sequential manner.

The optimal edges and durations are specified as follows. For the lth game over the interval $[\underline{t}_{2l-1}, \bar{t}_{2l}]$, the optimal strategies of the players according to the subgame perfect equilibrium principle are given by

$$(\mathcal{E}_{2l}^{\mathrm{D}*}, \delta_{2l}^{\mathrm{D}*}) \in \arg \max_{(\mathcal{E}_{2l}^{\mathrm{D}}, \delta_{2l}^{\mathrm{D}})} U_2^{\mathrm{D}}, \quad (11)$$

$$(\bar{\mathcal{E}}_{2l}^{\mathrm{A}*}, \mathcal{E}_{2l}^{\mathrm{A}*}, \delta_{2l}^{\mathrm{A}*}) \in \arg \max_{(\bar{\mathcal{E}}_{2l}^{\mathrm{A}}, \mathcal{E}_{2l}^{\mathrm{A}}, \delta_{2l}^{\mathrm{A}})} U_2^{\mathrm{A}}, \quad (12)$$

$$(\mathcal{E}_{2l-1}^{\mathrm{D}*}, \delta_{2l-1}^{\mathrm{D}*}) \in \arg \max_{(\mathcal{E}_{2l-1}^{\mathrm{D}}, \delta_{2l-1}^{\mathrm{D}})} U^{\mathrm{D}}, \quad (13)$$

$$(\bar{\mathcal{E}}_{2l-1}^{\mathrm{A}*}, \mathcal{E}_{2l-1}^{\mathrm{A}*}, \delta_{2l-1}^{\mathrm{A}*}) \in \arg \max_{(\bar{\mathcal{E}}_{2l-1}^{\mathrm{A}}, \mathcal{E}_{2l-1}^{\mathrm{A}}, \delta_{2l-1}^{\mathrm{A}})} U^{\mathrm{A}}, \quad (14)$$

with U_2^{A} and U_2^{D} being parts of U^{A} and U^{D} associated with the $(2l)$th interval, respectively. We assume that all parameters and utility functions are known to all players, including the energy parameters ($\kappa^{\mathrm{A}}, \rho^{\mathrm{A}}, \beta^{\mathrm{A}}$ and $\kappa^{\mathrm{D}}, \rho^{\mathrm{D}}, \beta^{\mathrm{D}}$) of the opposing player. This implies that a player is aware of the optimal strategies of other player, e.g., the defender knows which edges are optimally attacked by the attacker given the defender's best response.

Note that to find $(\bar{\mathcal{E}}_{2l-1}^{\mathrm{A}*}, \mathcal{E}_{2l-1}^{\mathrm{A}*}, \delta_{2l-1}^{\mathrm{A}*})$, one needs to obtain $(\mathcal{E}_{2l-1}^{\mathrm{D}*}(\bar{\mathcal{E}}_{2l-1}^{\mathrm{A}}, \mathcal{E}_{2l-1}^{\mathrm{A}}, \delta_{2l-1}^{\mathrm{A}}), \delta_{2l-1}^{\mathrm{D}*}(\bar{\mathcal{E}}_{2l-1}^{\mathrm{A}}, \mathcal{E}_{2l-1}^{\mathrm{A}}, \delta_{2l-1}^{\mathrm{A}}))$ beforehand. Likewise, to find $(\mathcal{E}_{2l-1}^{\mathrm{D}*}, \delta_{2l-1}^{\mathrm{D}*})$, one needs to obtain $(\bar{\mathcal{E}}_{2l}^{\mathrm{A}*}(\mathcal{E}_{2l-1}^{\mathrm{D}}, \delta_{2l-1}^{\mathrm{D}}), \mathcal{E}_{2l}^{\mathrm{A}*}(\mathcal{E}_{2l-1}^{\mathrm{D}}, \delta_{2l-1}^{\mathrm{D}}), \delta_{2l}^{\mathrm{A}*}(\mathcal{E}_{2l-1}^{\mathrm{D}}, \delta_{2l-1}^{\mathrm{D}}))$. These optimization problems are solved by the players at the start of the lth game, i.e., the strategies for the second part ($(2l)$th interval) are decided in the beginning of the $(2l-1)$th interval. The players are not able to further change their strategies for the $(2l)$th interval after it has been determined before at the start of the game. The agents' dynamics and the players' energy condition will affect the players' strategies in each game.

In this paper, we focus on the cluster formation over different intervals. We are able to find the optimal strategies of the players (11)–(14) by computing all possible combinations of edges and action durations, since they are both finite. It is also clear that the complexity of the game depends on the graph structure: it takes much longer to solve (11)–(14) in more complex graphs, since there are more possible combinations of edges.

III. Clustering and Consensus Analysis

In this section, we examine the effect of the attacker's energy model on the cluster formation and multiagent consensus.

We first discuss the defender's optimal strategy on some games with specific conditions.

Lemma 3.1: The defender always recovers in the $(2l)$th interval ($\mathcal{E}_{2l}^{\mathrm{D}} \neq \emptyset$), as long as $\mathcal{E}_{2l}^{\mathrm{A}} \neq \emptyset$.

From the result of $(2l)$th interval above, we are now able to state the result of $(2l_i - 1)$th interval for some l.

Lemma 3.2: There exists an infinite sequence $\bar{l} := \{\bar{l}_1, \bar{l}_2, \ldots\}$ of the game indexes where $\bar{l}_{i+1} > \bar{l}_i$ and $\bar{l}_i \in \mathbb{N}$ such that in the $(\bar{l}_i)$th game, the optimal strategy for the defender in the $(2\bar{l}_i - 1)$th attack interval is to recover from attacks with normal strength, i.e., $\mathcal{E}_{2\bar{l}_i-1}^{\mathrm{D}} \neq \emptyset$ as long as $\mathcal{E}_{2\bar{l}_i-1}^{\mathrm{A}} \neq \emptyset$.

The following result provides a necessary condition for

the agents to be separated into multiple clusters for infinitely long durations without achieving consensus. The results in Lemmas 3.1 and 3.2, which characterize the defender's optimal strategies in each interval of a game, enable us to derive the following result.

Proposition 3.3: The necessary condition to prevent the consensus from happening is $\bar{m}^{\mathrm{A}} \geq s\lambda$, with λ denoting the edge connectivity of $\mathcal{G}$.

However, the necessary condition in Proposition 3.3 is not sufficient for preventing consensus, since even with $\bar{m}^{\mathrm{A}}$ large enough, the attacker may decide to strongly attack fewer edges instead. This is related to the attacker's energy usage, as we see in the next section.

IV. Case Study on Attacker's Energy Usage

In this section, we investigate how the attacker uses its energy by comparing several attack strategies that characterize different energy consumption profiles. With the ability to use strong jamming signals, the attacker is able to prevent consensus by attacking some appropriate edges strongly at all times, with the downside that it consumes more energy. However, here we will show that under some conditions related to the energy usage, the attacker chooses not to attack edges strongly. While this attack strategy may be optimal according to U^{A} defined over interval $[\underline{t}_{2l-1}, \overline{t}_{2l}]$, it will be unsuccessful in preventing consensus.

Here, we discuss a special case where there are three agents (agents 1, 2, and 3) in a line/path graph 1–2–3. Specifically, we investigate the effect of different x_0 and different ρ^{A} to the clustering process. Throughout this section, we set $\delta = \beta^{\mathrm{A}} = \beta^{\mathrm{D}} = a = b = 1$, and $\kappa^{\mathrm{A}} = \gamma^{\mathrm{D}} = 0$. We choose this setting for simplicity, but we will see that the implications hold under other conditions.

A. Effect of Initial States x_0

Here we will investigate the effect of different initial states $x_0 = [x', 0, -x']^{\mathrm{T}}$ on the value of U^{A} in the first game ($l = 1$). We also set $\rho^{\mathrm{A}} = 2.5$, implying that $\bar{m}_{\mathrm{A}} = 2$. In this setting, the attacker has at least two strategy choices in $l = 1$: **(1a)** $|\bar{\mathcal{E}}_1^{\mathrm{A}}| = 1$, $|\mathcal{E}_1^{\mathrm{A}}| = 0$, and **(1b)** $|\bar{\mathcal{E}}_1^{\mathrm{A}}| = 0$, $|\mathcal{E}_1^{\mathrm{A}}| = 1$, with $\delta_1^{\mathrm{A}} = |\bar{\mathcal{E}}_2^{\mathrm{A}}| = |\mathcal{E}_2^{\mathrm{A}}| = 1$ in both cases. It is clear that in Case (1b) the attacker attacks fewer edges in the first part to save its energy that will be used in the second part. We assume that the defender with $\kappa^{\mathrm{D}} = 1$ and $\rho^{\mathrm{D}} = 0.5$ always recovers $\mathcal{E}_k^{\mathrm{A}}$. Other strategies are not discussed due to space limitation.

Case (1a): We notice that in this case $|\mathcal{E}_1^{\mathrm{D}}| = 0$, since $|\mathcal{E}_1^{\mathrm{A}}| = 0$. With the parameters specified above, we have $U^{\mathrm{A}} = z_1 + 4 + z_2\Delta_2^{\mathrm{A}} - (-4(\Delta_2^{\mathrm{A}} - \delta_2^{\mathrm{D}}) + c(\mathcal{G}_2^{\mathrm{D}})\delta_k^{\mathrm{D}})$. The value $c(\mathcal{G}_1^{\mathrm{A}}) = -4$ is from the fact that regardless of the attacked edges, there are always two clusters: one cluster has one agent and the other has two agents.

From $|\mathcal{E}_k^{\mathrm{A}}|$, $|\bar{\mathcal{E}}_k^{\mathrm{A}}|$, and $|\mathcal{E}_k^{\mathrm{D}}|$ above, we obtain $\Delta_2^{\mathrm{A}} = 1$ and $\Delta_2^{\mathrm{D}} = 3$. With $x_0 = [x', 0, -x']^{\mathrm{T}}$, if one agent is disconnected for $k = 1$, the function z_k becomes $z_1 = (e^{-2\delta}x')^2 + [((3 - e^{-2\delta})x')^2 + ((3 + e^{-2\delta})x')^2]/4$ from (1).

Now, since the defender recovers one edge for $k = 2$ (since $|\mathcal{E}_2^{\mathrm{A}}| = 1$), the graph for $k = 2$ is the same as that for $k = 1$: one agent gets disconnected from the other two. Finally, we substitute z_1 and z_2 into U^{A} and obtain

$$U^{\mathrm{A}} = \frac{3(1 + e^4 + 6e^8)(x')^2}{2e^8} + 8 \approx 9.028(x')^2 + 8. \quad (15)$$

Case (1b): Under the assumption that $|\mathcal{E}_1^{\mathrm{D}}| > 0$, we first obtain $\Delta_1^{\mathrm{D}} = 2$, which implies that $\delta_1^{\mathrm{D}} = \delta$ and as a result $c(\mathcal{G}_1^{\mathrm{D}}) = 0$. Therefore, we have $U^{\mathrm{A}} = z_1 + z_2\Delta_2^{\mathrm{A}} - (c(\mathcal{G}_2^{\mathrm{A}})(\Delta_2^{\mathrm{A}} - \delta_2^{\mathrm{D}}) + c(\mathcal{G}_2^{\mathrm{D}})\delta_2^{\mathrm{D}})$. We then obtain $\Delta_2^{\mathrm{A}} = 3$, which is longer than in Case (1a) above since in this case the attacker is using less energy for $k = 1$, and $\Delta_2^{\mathrm{D}} = 1$, which is shorter than in Case (1a) for the similar reason.

Since the graph remains connected for $k = 1$, from (1) we obtain z_k where all agents are connected in the path graph as $z_1 = 6(e^{-\delta}x')^2$, with the agents' states becoming $x(t) = [e^{-t}x',\ 0,\ -e^{-t}x']^{\mathrm{T}}$. We substitute z_k in U^{A} to get

$$U^{\mathrm{A}} = \frac{3(3 + 13e^4)(x')^2}{2e^6} + 16 \approx 2.650(x')^2 + 16. \quad (16)$$

We then compare (15) and (16) to obtain a condition on x' for selecting strategies. Specifically, the attacker's strategy $|\bar{\mathcal{E}}_1^{\mathrm{A}}| = 1, |\mathcal{E}_1^{\mathrm{A}}| = 0$ is better than $|\bar{\mathcal{E}}_1^{\mathrm{A}}| = 0, |\mathcal{E}_1^{\mathrm{A}}| = 1$ if $x' > 1.12$. Otherwise, the strategy in Case (1b) is better.

This example shows that the initial state x_0 influences the players' strategies. In general, the attacker tends to save its energy in the first part by attacking fewer edges, if the agents' states are sufficiently close. This implies that consensus may still happen if the attacker does not attack with strong jamming signals, despite with high enough $\bar{m}^{\mathrm{A}}$.

B. Effect of Attacker's Recharge Rate ρ^{A} (Smaller $\bar{m}^{\mathrm{A}}$)

We next investigate U^{A} with varying ρ^{A}. Here we set $2 < \rho^{\mathrm{A}} < 3$, and we also assume that κ^{D} and ρ^{D} are large enough so that $\delta_k^{\mathrm{D}} = \delta_k^{\mathrm{A}}$ for any k. We again compare two cases of strategy choices as above: **(2a)** $|\bar{\mathcal{E}}_1^{\mathrm{A}}| = 1$, $|\mathcal{E}_1^{\mathrm{A}}| = 0$, and **(2b)** $|\bar{\mathcal{E}}_1^{\mathrm{A}}| = 0$, $|\mathcal{E}_1^{\mathrm{A}}| = 1$, with $\delta_1^{\mathrm{A}} = |\bar{\mathcal{E}}_2^{\mathrm{A}}| = |\mathcal{E}_2^{\mathrm{A}}| = 1$ in both cases. Here we assume that $x_0 = [1, 0, -1]^{\mathrm{T}}$.

Case (2a): The utility function here is $U^{\mathrm{A}} = z_1 + 4 + z_2\Delta_2^{\mathrm{A}} - (-4(\Delta_2^{\mathrm{A}} - \delta_2^{\mathrm{D}}) + c(\mathcal{G}_2^{\mathrm{D}})\delta_2^{\mathrm{D}})$. From $|\mathcal{E}_1^{\mathrm{A}}|$ and $|\bar{\mathcal{E}}_1^{\mathrm{A}}|$, we obtain $\Delta_2^{\mathrm{A}} = \frac{\rho^{\mathrm{A}}-2}{3-\rho^{\mathrm{A}}}$, z_1, and z_2, resulting in $U^{\mathrm{A}} = \frac{3(3+e^{-4})}{2} + 4 + \frac{\rho^{\mathrm{A}}-2}{3-\rho^{\mathrm{A}}}\left(\frac{3(3+e^{-4(\frac{\rho^{\mathrm{A}}-2}{3-\rho^{\mathrm{A}}})})}{2} + 4\right)$.

Case (2b): Since the graph remains connected for $k = 1$, we obtain $z_1 = 6e^{-2}$, with $x(\underline{t}_2) = [e^{-1},\ 0,\ -e^{-1}]$. Since the defender recovers and hence one agent is disconnected from the other agents for the entire Δ_2^{A}, we use the same approach as in Cases (1a) and (1b) to obtain the value of z_2. We then obtain $U^{\mathrm{A}} = 6e^{-2} + \frac{\rho^{\mathrm{A}}-1}{3-\rho^{\mathrm{A}}}\left(\frac{3(3+e^{-4(\frac{\rho^{\mathrm{A}}-1}{3-\rho^{\mathrm{A}}})})}{2e^2} + 4\right)$. From two U^{A} above, the attacker's strategy in Case (2a) is better than the one in Case (2b) if $\rho^{\mathrm{A}} < 2.812$.

We note that from this example, the higher the attacker's recharge rate ρ^{A} is, the more likely the attacker attacks fewer edges in the first part. This has an interesting implication, where the consensus is more likely to happen for some higher ρ^{A}. This is because the attack duration δ_k^{A} contributes much to the value of U^{A}, where δ_k^{A} is multiplied by z_k.

C. Effect of Attacker's Recharge Rate ρ^{A} (Larger $\bar{m}^{\mathrm{A}}$)

We now discuss a scenario with varying ρ^{A} and higher $\bar{m}^{\mathrm{A}}$, compared to Cases (1b) and (2b) above. Specifically,

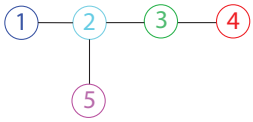

Fig. 4. Graph used for simulations in Section V

we set $3 < \rho^{\mathrm{A}} < 4$, implying $\bar{m}_{\mathrm{A}} = 3$. We also assume that the defender has enough energy to recover all possible $\mathcal{E}_k^{\mathrm{A}}$ for δ_k^{A} at any kth interval. The initial states are $x_0 = [1, 0, -1]^{\mathrm{T}}$. The compared strategies are: **(3a)** $|\bar{\mathcal{E}}_1^{\mathrm{A}}| = 1$, $|\mathcal{E}_1^{\mathrm{A}}| = 0$, and **(3b)** $|\bar{\mathcal{E}}_1^{\mathrm{A}}| = 0$, $|\mathcal{E}_1^{\mathrm{A}}| = 1$, with $\delta_1^{\mathrm{A}} = 1$, $|\bar{\mathcal{E}}_2^{\mathrm{A}}| = 2$, and $|\mathcal{E}_2^{\mathrm{A}}| = 0$ in both cases.

With the same approach as in Cases (2a) and (2b) above, we obtain for Case (3a) $U^{\mathrm{A}} = \frac{3(3+e^{-4})}{2} + 4 + \frac{\rho^{\mathrm{A}}-2}{4-\rho^{\mathrm{A}}}\left(\frac{3(3+e^{-4})}{2} + 6\right)$, and for Case (3b) $U^{\mathrm{A}} = 6e^{-2} + \frac{\rho^{\mathrm{A}}-1}{4-\rho^{\mathrm{A}}}\left(6e^{-2}+6\right)$. By comparing these, we observe that for any value of ρ^{A} with $3 < \rho^{\mathrm{A}} < 4$, the attacker's strategy in Case (3a) is always better. This shows that attacking with stronger signals, which may prevent consensus, may be better for the attacker if $\bar{m}^{\mathrm{A}}$ is large enough.

V. Numerical Simulation of Dynamic Games: Effect of Attacker's Recharge Rate ρ^{A}

In our simulations, we use the graph shown in Fig. 4 with five vertices/agents with parameters $\beta^{\mathrm{A}} = 1.1$, $\beta^{\mathrm{D}} = 0.6$, $\kappa^{\mathrm{A}} = 0$, $\kappa^{\mathrm{D}} = 5$, $\rho^{\mathrm{D}} = 0.5$, $\gamma^{\mathrm{D}} = 0.1$, $a = 0.1$, $b = 1$, and $x_0 = [1.8, 5.2, 0.1, 2.7, 2.0]^{\mathrm{T}}$. Figs. 5 and 6 show the states of the agents with $\rho^{\mathrm{A}} = 5$ and $\rho^{\mathrm{A}} = 2.5$, respectively. Since $\lambda = 1$ in this graph, note that ρ^{A} in both simulations satisfy the condition needed in order not to achieve consensus in Proposition 3.3. The line colors in Figs. 5 and 6 correspond to the colors of the agents in Fig. 4. In Figs. 5 and 6 discussed in this section, the vertical blue lines indicate the end time of each part (attack interval), with the dashed lines indicating the end times of the first parts, and the solid lines indicating the end times of the second part of the games.

In the first simulation, we have $\bar{m}^{\mathrm{A}} = \lfloor \rho^{\mathrm{A}}/\beta^{\mathrm{A}} \rfloor = 4$, whereas $\bar{m}^{\mathrm{A}} = 2$ in the second simulation. This has an impact on the consensus, where in the second simulation consensus is achieved although the attacker has the capability to disconnect an agent with strong jamming signals. On the other hand, in the first simulation, agents are divided into different clusters and do not converge to the same state.

VI. Conclusion and Future Works

We have formulated a two-player game in a cybersecurity problem of multiagent systems, where the players consider the impact of their actions on future communication topology and future agent states. The optimal strategies of the players have been analyzed. We have also discussed the impact of initial agent states $x(0)$ and the attacker's recharge rate ρ^{A} on cluster formation among agents. Possible future works include considering the more dynamic rolling horizon approach, where players may change their strategies (that have been determined beforehand) at several points in time, in order to adapt to the changing condition of the systems.

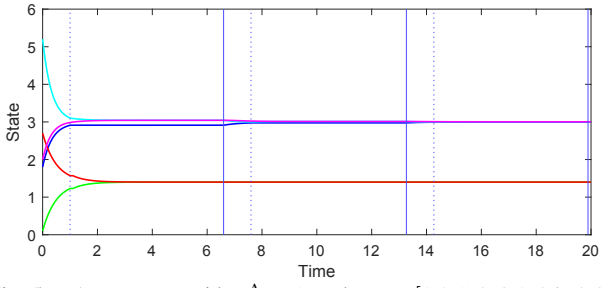

Fig. 5. Agent states with $\rho^{\mathrm{A}} = 5$ and $x_0 = [1.8, 5.2, 0.1, 2.7, 2.0]^{\mathrm{T}}$. Here, the agents are divided into different parts: agents 1,2,5 have the same states, separated from agents 3 and 4 in the different cluster.

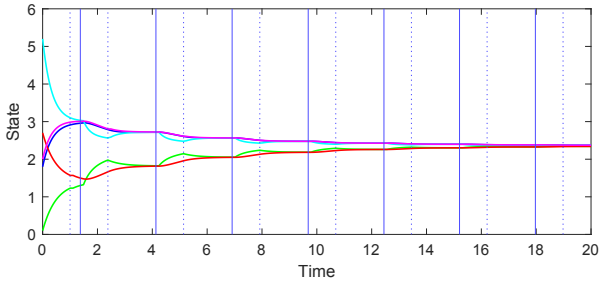

Fig. 6. Agent states with $\rho^{\mathrm{A}} = 2.5$. The agents achieve consensus here.

References

[1] F. Bullo, *Lectures on Network Systems*. Kindle Direct Publishing, 2019.

[2] H. Sandberg, S. Amin, and K. H. Johansson, "Special issue on cyberphysical security in networked control systems," *IEEE Control Syst. Mag.*, vol. 35, pp. 20–23, 2015.

[3] T. Alpcan and T. Basar, *Network Security: A Decision and Game-Theoretic Approach*. Cambridge University Press, 2010.

[4] M. Pirani, E. Nekouei, H. Sandberg, and K. Johansson, "A graph-theoretic equilibrium analysis of attacker-defender game on consensus dynamics under $\mathcal{H}_2$ performance metric," *IEEE Trans. Netw. Sci. Eng.*, to appear, 2020. Online, https://ieeexplore.ieee.org/document/9250594.

[5] D. Senejohnny, P. Tesi, and C. De Persis, "A jamming resilient algorithm for self-triggered network coordination," *IEEE Trans. Control Netw. Syst.*, vol. 5, pp. 981–990, 2018.

[6] A. Cetinkaya, K. Kikuchi, T. Hayakawa, and H. Ishii, "Randomized transmission protocols for protection against jamming attacks in multi-agent consensus," *Automatica*, vol. 117, 2020.

[7] A. Cetinkaya, H. Ishii, and T. Hayakawa, "Networked control under random and malicious packet losses," *IEEE Trans. Autom. Contr.*, vol. 62, pp. 2434–2449, 2017.

[8] ——, "The effect of time-varying jamming interference of networked stabilization," *SIAM J. Control Optim.*, vol. 56, pp. 2398–2435, 2018.

[9] Y. Nugraha, A. Cetinkaya, T. Hayakawa, H. Ishii, and Q. Zhu, "Dynamic resilient network games with applications to multiagent consensus," *IEEE Trans. Control Netw. Syst.*, vol. 8, pp. 246–259, 2021.

[10] J. Chen, C. Touati, and Q. Zhu, "A dynamic game approach to strategic design of secure and resilient infrastructure network," *IEEE Trans. Inf. Forensics Security*, vol. 15, pp. 462–474, 2020.

[11] C. Altafini, "Consensus problems on networks with antagonistic interactions," *IEEE Trans. Autom. Contr.*, vol. 58, no. 4, pp. 935–946, 2013.

[12] G. D. Pasquale and M. E. Valcher, "Consensus for clusters of agents with cooperative and antagonistic relationships," arXiv: 2008.12398, 2020.

[13] D. Yang, G. Xue, J. Zhang, A. Richa, and X. Fang, "Coping with a smart jammer in wireless networks: A Stackelberg game approach," *IEEE Trans. Wireless Commun.*, vol. 12, pp. 4038–4047, 2013.

[14] M. A. Maleki Sadr, M. Ahmadian-Attari, R. Amiri, and V. V. Sabegh, "Worst-case jamming attack and optimum defense strategy in cooperative relay networks," *IEEE Control Systems Letters*, vol. 3, no. 1, pp. 7–12, 2019.

[15] M. L. Katz and C. Shapiro, "Systems competition and network effects," *Journal of Economic Perspective*, vol. 8, pp. 93–115, 1994.

[16] Y. Nugraha, A. Cetinkaya, T. Hayakawa, H. Ishii, and Q. Zhu, "Dynamic resilient graph games for state-dependent jamming attacks analysis on multi-agent systems," in *Proc. IFAC World Congress*, 2020, pp. 3421–3426.